ACOUSTIC-ELASTIC COUPLED FULL-WAVEFORM INVERSION IN THE LAPLACE DOMAIN WITH SCALED GRADIENT FOR IMPROVED DENSITY RECOVERY

SEUNG-GOO KANG[1], UGEUN JANG[1*], HAN-JOON KIM[2], HYEONG-TAE JOU[2], CHANGSOO SHIN[3], JONG KUK HONG[1] and YOUNG KEUN JIN[1]

[1] Division of Polar Earth-System Sciences, Korea Polar Research Institute, Incheon 21990, South Korea. ugeun.jang@kopri.re.kr
[2] Korean Seas Geosystem Research Unit, Korea Institute of Ocean Science and Technology, Busan, 49111, South Korea.
[3] Department of Energy Systems Engineering, Seoul National University, Seoul 08826, South Korea.

(Received September 21, 2017; revised version accepted August 5, 2018)

ABSTRACT

Kang, S.-G., Jang, U., Kim, H.-J., Jou, H.-T., Shin, C.S., Hong, J.K. and Jin, Y.K., 2018. Acoustic-elastic coupled full-waveform inversion in the Laplace domain with scaled gradient for improved density recovery. *Journal of Seismic Exploration*, 27: 487-504.

Acoustic-elastic coupled full-waveform inversion in the Laplace domain is well suited for recovering P- and S-wave velocity (V_P and V_S, respectively), and density from marine seismic data because it can simulate waves that are generated in the fluid (sea water) and propagate into the solid (seafloor). However, density is not recovered as reliably as V_P and V_S. In this study, we show that the density recovery procedure using full-waveform inversion for acoustic-elastic coupled media can be improved by scaling the gradient for the steepest descent operation. Gradient scaling is a heuristic approach that multiplies the gradient by the square of the gradient summed in the depth direction. We found that this scaling scheme resulted in more accurate density as well as attenuated numerical artefacts. To validate the scaling scheme, we illustrate both synthetic and real data examples.

KEY WORDS: Laplace domain, full-waveform inversion, density, gradient scaling, acoustic-elastic coupled wave equation.

0963-0651/18/$5.00

INTRODUCTION

Full-waveform inversion (FWI) computes the physical properties of the complicated subsurface from information brought to the surface by seismic waves which are recorded at the surface. Classical FWI includes the minimization of an objective function of the difference between the observed and modelled data. The minimization of the objective function is commonly performed using the steepest descent method (e.g., Shipp and Singh, 2002).

For reflection data, the narrow range of reflection angle apertures only allows the recovery of short wavelengths, resulting in insufficient low-frequency information (e.g., Symes, 2008). In addition, FWI is limited by local minima encountered during optimization. The Laplace-domain FWI, which uses the zero-frequency component of a damped wavefield, provides one possible solution for these limitations (Shin and Cha, 2008). Bae et al. (2010) derived an acoustic-elastic coupled FWI in the Laplace domain. Their method enables accurate computation of the subsurface from marine seismic data because it can deal with density as well as the S-wave generated below the seafloor. The velocities of P- and S-waves, given by V_P and V_S, respectively, are properly reconstructed by FWI. Compared with V_P and V_S, however, density is more difficult to reconstruct (Bae et al., 2010; Kang et al., 2012). Kang et al., (2016) proposed the gradient scaling function for FWI for acoustic-elastic coupled media in the Laplace domain and shows that a gradient scaling function can be used to construct more suitable P- and S-wave velocity inverted velocity model than previous method. Scaled Laplace gradient direction of the P- and S-wave velocities which were generated by the accumulated sum of the squares of the conventional gradient with respect to depth can improve the image of high-velocity structures and remove the numerical artifacts near the seafloor. However, they did not refer to the density inverse problems.

In this study, we demonstrate that the accuracy of reconstructed density can be improved by modifying the gradient direction of the objective function using scaling method (Kang et al., 2016) for acoustic-elastic coupled FWI in the Laplace domain. The density gradient was empirically modified and optimized through numerical tests. From the results of these tests, we infer that the density reconstruction is improved using the gradient scaled method, which proposed by Kang et al. (2016) for density only. Our discussion involves examples with both synthetic and real data.

FWI for acoustic-elastic coupled media in the Laplace domain

In this acoustic-elastic system, the wave propagation in water column (fluid media) is described in the acoustic wave equation, whereas the wave propagation under the seafloor (solid media) is described in the elastic wave equation. Two-dimensional acoustic wave equation in the Laplace domain can be defined as

$$-\frac{s^2}{c^2}\tilde{p}=\frac{\partial^2\tilde{p}}{\partial x^2}+\frac{\partial^2\tilde{p}}{\partial z^2}+\tilde{f} \quad , \tag{1}$$

where $\tilde{p}=\tilde{p}\left(x,z,s\right)$ is the Laplace domain pressure-field in water column (fluid media); s is the damping coefficient of the Laplace transform, $c\left(x,z\right)=\sqrt{k/\rho_A}$ is velocity in water column (fluid media); k and ρ_A are the bulk modulus and density of water column (fluid media), respectively; and $\tilde{f}=\tilde{f}\left(x,z,s\right)$ is a source term.

In heterogeneous and isotropic solid media, two-dimensional elastic wave equation in the Laplace domain is written as

$$-\rho_E s^2\tilde{h}=\frac{\partial}{\partial x}\left((\lambda+2\mu)\frac{\partial\tilde{h}}{\partial x}+\lambda\frac{\partial\tilde{v}}{\partial z}\right)+\frac{\partial}{\partial z}\left(\mu\left(\frac{\partial\tilde{v}}{\partial x}+\frac{\partial\tilde{h}}{\partial z}\right)\right) \quad , \tag{2}$$

$$-\rho_E s^2\tilde{v}=\frac{\partial}{\partial x}\left(\mu\left(\frac{\partial\tilde{v}}{\partial x}+\frac{\partial\tilde{h}}{\partial z}\right)\right)+\frac{\partial}{\partial z}\left(\lambda\frac{\partial\tilde{h}}{\partial x}+(\lambda+2\mu)\frac{\partial\tilde{v}}{\partial z}\right) \quad , \tag{3}$$

where ρ_E is the density in solid media; λ and μ are the Lamé constants; and $\tilde{h}=\tilde{h}\left(x,z,s\right)$ and $\tilde{v}=\tilde{v}\left(x,z,s\right)$ are the horizontal and vertical displacements, respectively.

In acoustic-elastic coupled media, pressure fields generated in water column are converted to horizontal and vertical particle displacements at the seafloor, which propagate through the seafloor as the elastic medium. The interface boundaries between fluid and solid media should meet the continuity conditions (Zienkiewicz et al., 2005; Komatitsch et al., 2000) as follows:

$$\nabla\tilde{p}\cdot\mathbf{n}=-\rho_A\ddot{\mathbf{u}}_E\cdot\mathbf{n} \quad , \tag{4}$$

and

$$\sigma\cdot\mathbf{n}=-\tilde{p}\mathbf{n} \quad , \tag{5}$$

where $\ddot{\mathbf{u}}_E$ is the second derivative of the displacement vector with respect to time, $\mathbf{n}$ is the normal vector from the interface and σ is the symmetric, second-ordered stress tensor. When the elastic waves are reflected and return to the seafloor, they are converted to pressure fields and then propagate to the sea surface.

Following the finite element method (FEM) by Kang et al. (2012), we can obtain a discretized finite element equation for acoustic-elastic coupled media, which considers the irregular seafloor geometry. The coupled media equation with interface conditions can be expressed in matrix form in the Laplace domain as

$$\begin{pmatrix} \mathbf{K}^A + s^2/c^2\,\mathbf{M}^A & \rho_A s^2 \mathbf{Q}^A \sin\theta & \rho_A s^2 \mathbf{Q}^A \cos\theta \\ \left[\mathbf{Q}^E\right]^T \sin\theta & \mathbf{K}^{11} - \rho_E s^2 \mathbf{M}^{11} & \mathbf{K}^{12} \\ \left[\mathbf{Q}^E\right]^T \cos\theta & \mathbf{K}^{21} & \mathbf{K}^{22} - \rho_E s^2 \mathbf{M}^{22} \end{pmatrix} \begin{pmatrix} \tilde{\mathbf{p}}(s) \\ \tilde{\mathbf{v}}_x(s) \\ \tilde{\mathbf{v}}_z(s) \end{pmatrix} = \begin{pmatrix} \tilde{\mathbf{f}}(s) \\ 0 \\ 0 \end{pmatrix}, \quad (6)$$

where $\mathbf{K}^A$ is the stiffness matrix for acoustic media; $\mathbf{K}^{11}$, $\mathbf{K}^{12}$, $\mathbf{K}^{21}$, and $\mathbf{K}^{22}$ are the stiffness matrices for elastic media; $\mathbf{M}^A$ designates the mass matrix for acoustic media; $\mathbf{M}^{11}$ and $\mathbf{M}^{22}$ are the mass matrices for elastic media; and $\mathbf{Q}^A$ and $\mathbf{Q}^E$ are the interface boundary matrices in acoustic and elastic media, respectively. Furthermore, θ is the slope of the interface between the acoustic and elastic layers, $\tilde{\mathbf{p}}(s)$ is a pressure field vector, $\tilde{\mathbf{v}}_x(s)$ and $\tilde{\mathbf{v}}_z(s)$ are the horizontal and vertical displacements in the Laplace domain for elastic media, respectively, and $\tilde{\mathbf{f}}(s)$ is the Laplace-domain source vector (Kang et al., 2012).

We can simplify (1) using an impedance matrix **S**:

$$\mathbf{S}\tilde{\mathbf{u}} = \tilde{\mathbf{f}}, \quad (7)$$

where $\tilde{\mathbf{u}}$ is the Laplace-domain wavefield vector containing the pressure field and the displacement. In acoustic-elastic coupled media, the Lamé constants (λ and μ) and density (ρ_E) are elastic model parameters which are updated by waveform inversion. After updating, these parameters are converted to V_P and V_S. In other words, the coupled media FWI can reconstruct the V_P, V_S, and density models.

In the FWI algorithm, the residual is measured by the difference between observed and modelled data. In the Laplace domain, the wavefield has very small absolute values, compared with those in the frequency domain (Shin and Cha, 2008). Therefore, for measuring the residuals of damped wavefields, the logarithmic objective function (Shin and Min, 2006) is more useful than the conventional l_2 objective function. The logarithmic objective function for Laplace-domain waveform inversion at a given Laplace damping constant is

$$E\left(k_{(ix,iz)}\right)=\frac{1}{2}\sum_{i=1}^{n_s}\sum_{j=1}^{n_r}\delta\tilde{r}_{ij}\delta\tilde{r}_{ij} \quad , \tag{8}$$

where

$$\delta\tilde{r}_{ij}=\ln(\frac{\tilde{u}_{ij}}{\tilde{d}_{ij}}) \quad . \tag{9}$$

In the above equations, $\tilde{d}_{ij}$, $\tilde{u}_{ij}$, and $\delta\tilde{r}_{ij}$ are the observed wavefield, the modelled wavefield, and the residual at the j^{th} receiver by the i^{th} source, respectively. The values n_s and n_r are the total number of sources and receivers, respectively. Using the back-propagation algorithm (e.g., Pratt et al., 1998), we can effectively calculate the gradient of the objective function with respect to the model parameter $k_{(ix,iz)}$ using the impedance matrix of the coupled wave equation **S** as

$$\nabla_{k_{(ix,iz)}}\mathbf{E}\left(ix,iz\right)=\mathrm{Re}\left[\sum_{i=1}^{n_s}(\mathbf{v}_{k_{(ix,iz)}})^T\mathbf{S}^{-1}\delta\tilde{\mathbf{r}}_i\right], \tag{10}$$

where $k_{(ix,iz)}$ represents all of the elastic model parameters (the Lamé constants and density) in the conventional algorithm. Here, $\mathbf{v}_{k_{(ix,iz)}}$ is the virtual source term defined as

$$\mathbf{v}_{k_{(ix,iz)}}=-\frac{\partial\mathbf{S}}{\partial k_{(ix,iz)}}\tilde{\mathbf{u}}_i, \tag{11}$$

where $\tilde{\mathbf{u}}_i$ is the forward modelled wavefield, and $\delta\tilde{\mathbf{r}}_i$ is the residual for the *i*-th source defined as

$$\delta\tilde{\mathbf{r}}_i=\begin{bmatrix}\ln(\tilde{u}_{i1}/\tilde{d}_{i1})/u_{i1}\\ \ln(\tilde{u}_{i2}/\tilde{d}_{i2})/u_{i2}\\ \vdots\\ \ln(\tilde{u}_{i,nr}/\tilde{d}_{i,nr})/u_{i,nr}\\ 0\\ \vdots\\ 0\end{bmatrix}. \tag{12}$$

After calculating the gradient of the objective function, all of the elastic model parameters in the coupled media are simultaneously updated as

$$k_{(ix,iz)}^{l+1} = k_{(ix,iz)}^{l} - \alpha^{l} \sum_{s=1}^{ns} NRM \left[\frac{\nabla_{k_{(ix,iz)}} \mathbf{E}(ix,iz)}{\sum_{i=1}^{n_s} (\mathbf{v}_{k_{(ix,iz)}})^{T} \cdot \mathbf{v}_{k_{(ix,iz)}} + \eta} \right], \tag{13}$$

where l is the iteration number, α^{l} is the step size parameter at the l-th iteration, ns is the total number of Laplace damping constants, NRM is a normalizing operator, and η is a stabilizing factor. We estimate the unknown source wavelet from the initial source using Newton's method (Shin et al., 2007). We repeat this procedure until a stopping criterion is met.

DENSITY RECONSTRUCTION BY FWI WITH GRADIENT SCALING METHOD

FWI in the Laplace-domain for acoustic-elastic coupled media frequently computes V_P and V_S models with the density model fixed (Bae et al., 2010) because computational stability of density is difficult to achieve (Tarantola, 1986). In this study, the Lamé constants (λ and μ) and density are updated separately until convergence has been achieved. In other words, the Lamé constants are updated with density fixed for the first 10 iterations, and then with the previously updated Lamé constants fixed, density is updated for the next 10 iterations. During the density updates, the scaled density gradient (Kang et al., 2016) was employed. The scaled gradient is computed by the vertically accumulated squared sum of the original density gradient values. The accumulated density gradient $\nabla_{density_{(ix,iz)}} \mathbf{E}_{acc}(ix,iz)$ is calculated as

$$\begin{aligned} \nabla_{density_{(ix,iz)}} \mathbf{E}_{acc}(ix,iz) &= \nabla_{density_{(ix,iz)}} \mathbf{E}_{acc}(ix,iz-1) \\ &\quad + \left[\nabla_{density_{(ix,iz)}} \mathbf{E}(ix,iz) \right]^2, \quad ix = 1,\cdots,nx, \quad iz = 2,\cdots,nz, \end{aligned} \tag{14}$$

where $\mathbf{v}_{density_{(ix,iz)}}$ is the virtual source term for the density.

After obtaining the accumulated density gradient $\nabla_{density_{(ix,iz)}} \mathbf{E}_{acc}(ix,iz)$, we compute the scaled gradient $\nabla_{density_{(ix,iz)}} \mathbf{E}_{\mathbf{L}}(ix,iz)$ by multiplying the conventional gradient and the accumulated gradient:

$$\nabla_{density(ix,iz)} \mathbf{E}_L(ix,iz) = \nabla_{density(ix,iz)} \left[\mathbf{E}(ix,iz) \cdot \mathbf{E}_{acc}(ix,iz) \right]. \tag{15}$$

Density is updated by the process:

$$density^{l+1}_{(ix,iz)} = density^{l}_{(ix,iz)} - \alpha^l \sum_{s=1}^{nf} NRM \left[\frac{\nabla_{density_{(ix,iz)}} \mathbf{E}_{\mathbf{L}}(ix,iz)}{\sum_{i=1}^{n_s} (\mathbf{v}_{density_{(ix,iz)}})^T \cdot \mathbf{v}_{density_{(ix,iz)}} + \eta} \right]. \tag{16}$$

Our FWI procedure consists of the following two steps: (1) V_P and V_S are updated with the initial density fixed for the first 10 iterations, and (2) density is updated for the next 10 iterations using the modified gradient, while keeping the previously updated V_P and V_S values fixed. These two steps are repeated until convergence has been achieved.

EXPERIMENTS WITH SYNTHETIC AND REAL DATA

Synthetic data example

We examine the results of FWI with the scaled gradient of density for Hess salt model. Fig. 1 shows Hess model (V_P , V_S, and density) that includes sea water and the irregular seafloor; below the seafloor, the salt body was modelled by higher V_P (4.51 km/s) and V_S (2.17 km/s) and lower density (2.16 g/cc) than the surrounding sediments. The synthetic data from Hess model consist of 164 shots with 851 receivers. The shot and receiver intervals are 100 m and 20 m, respectively. Fig. 2 shows the initial model for FWI in the Laplace domain. In this initial model, V_P, V_S, and density in sea water are 1.5 km/s, 0 km/s, and 1 g/cc, respectively. Below the seafloor, V_P, V_S, and density linearly increase to the depth of 3 km: V_P increases from 2.1 to 3.6 km/s, V_S increases from 1.2 to 2.2 km/s, and density increase from 2.1 to 3.0 g/cc. Fig. 3 shows the gradients of the Lamé constants (λ and μ) and density for updating the final models, which were calculated by the back-propagation algorithm in the Laplace domain (Bae et al., 2010). In the inversion process, we used 15 damping constants ranging from 1 to 15.

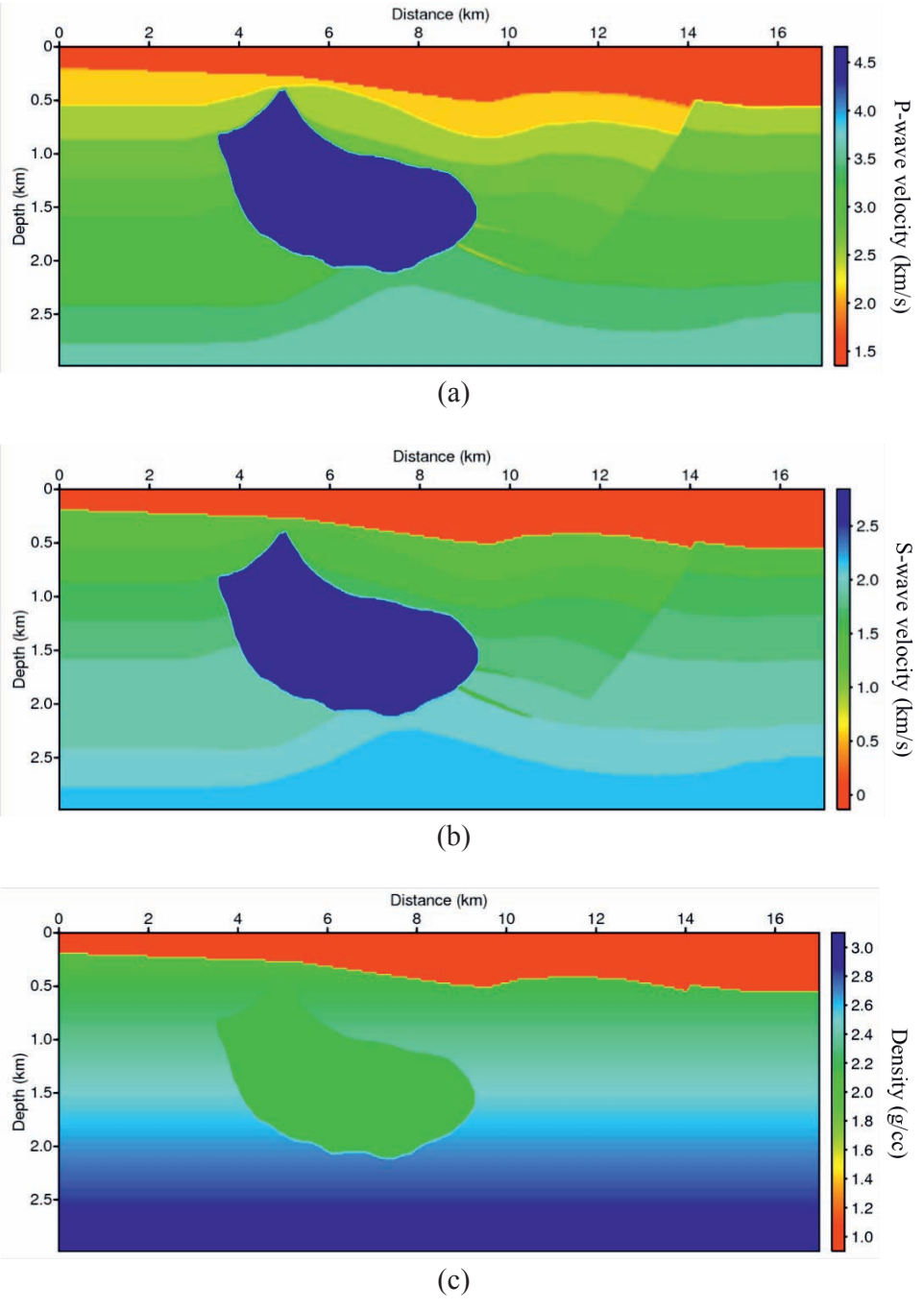

Fig. 1. Hess salt model: (a) V_P, (b) V_S, and (c) density.

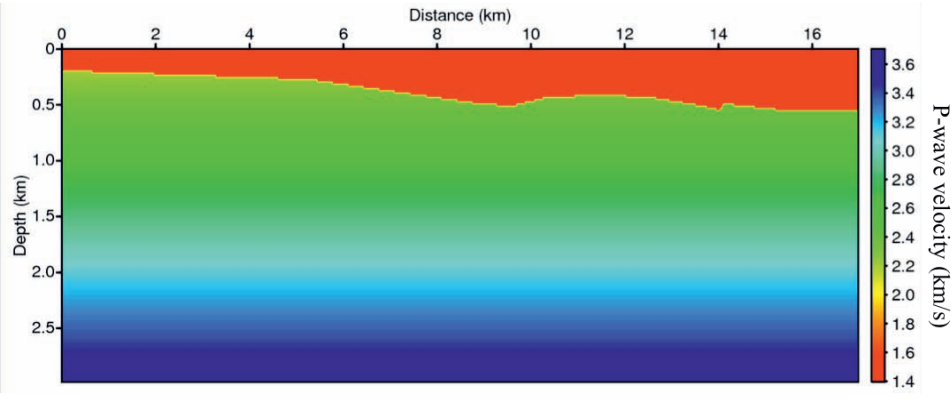

(a)

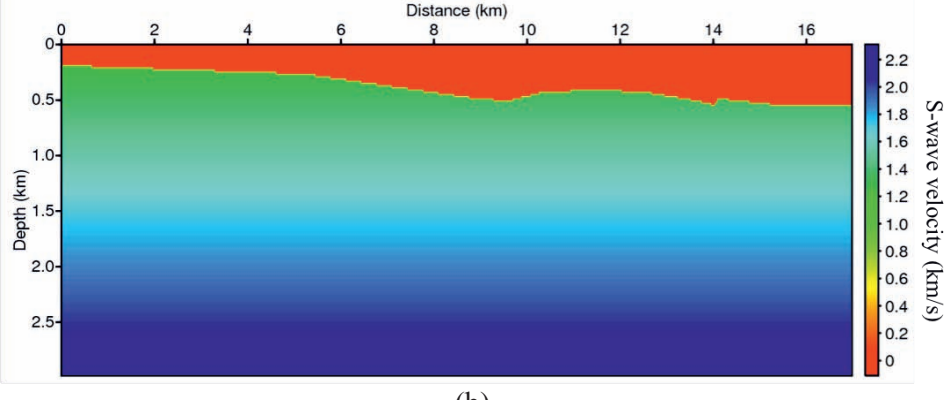

(b)

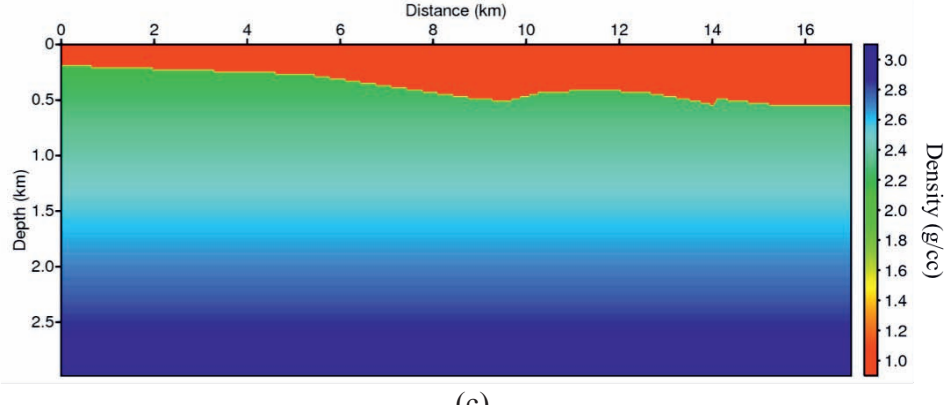

(c)

Fig. 2. The initial models for FWI of Hess salt model: (a) V_P, (b) V_S, and (c) density.

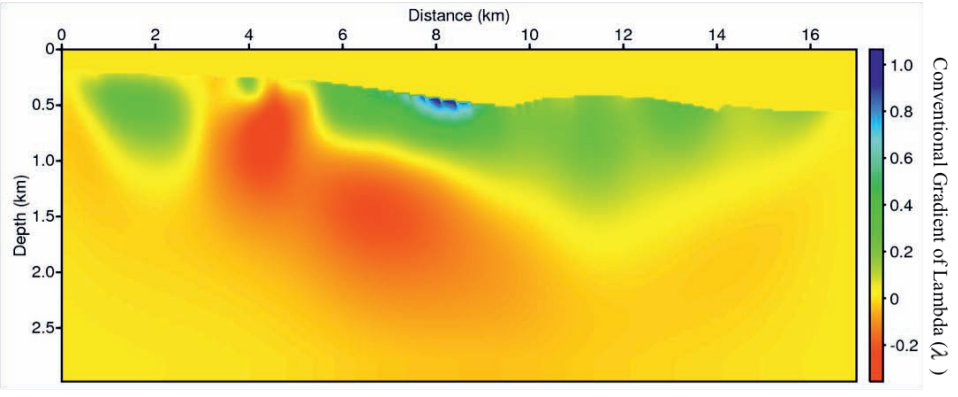

(a)

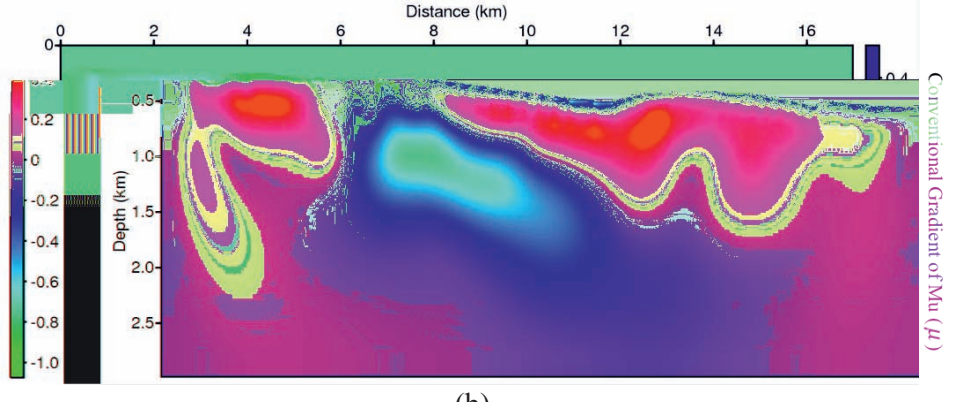

(b)

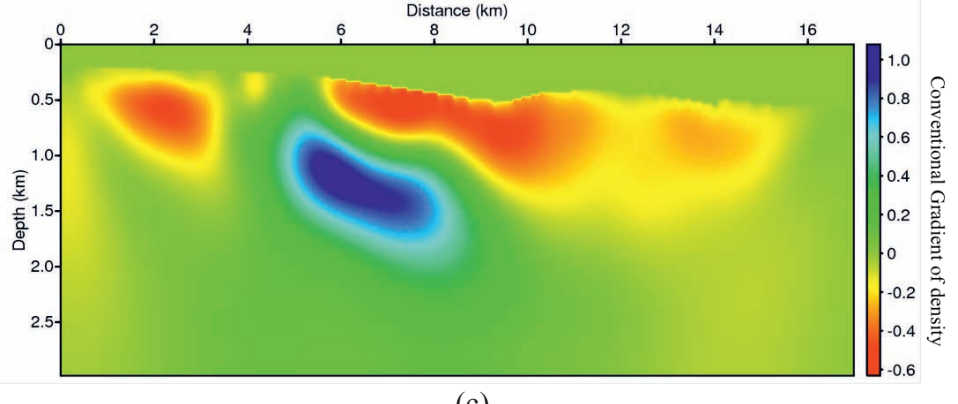

(c)

Fig. 3. The gradients of (a) λ, (b) μ, and (c) density after 51 iterations. The gradients were calculated by the back-propagation algorithm.

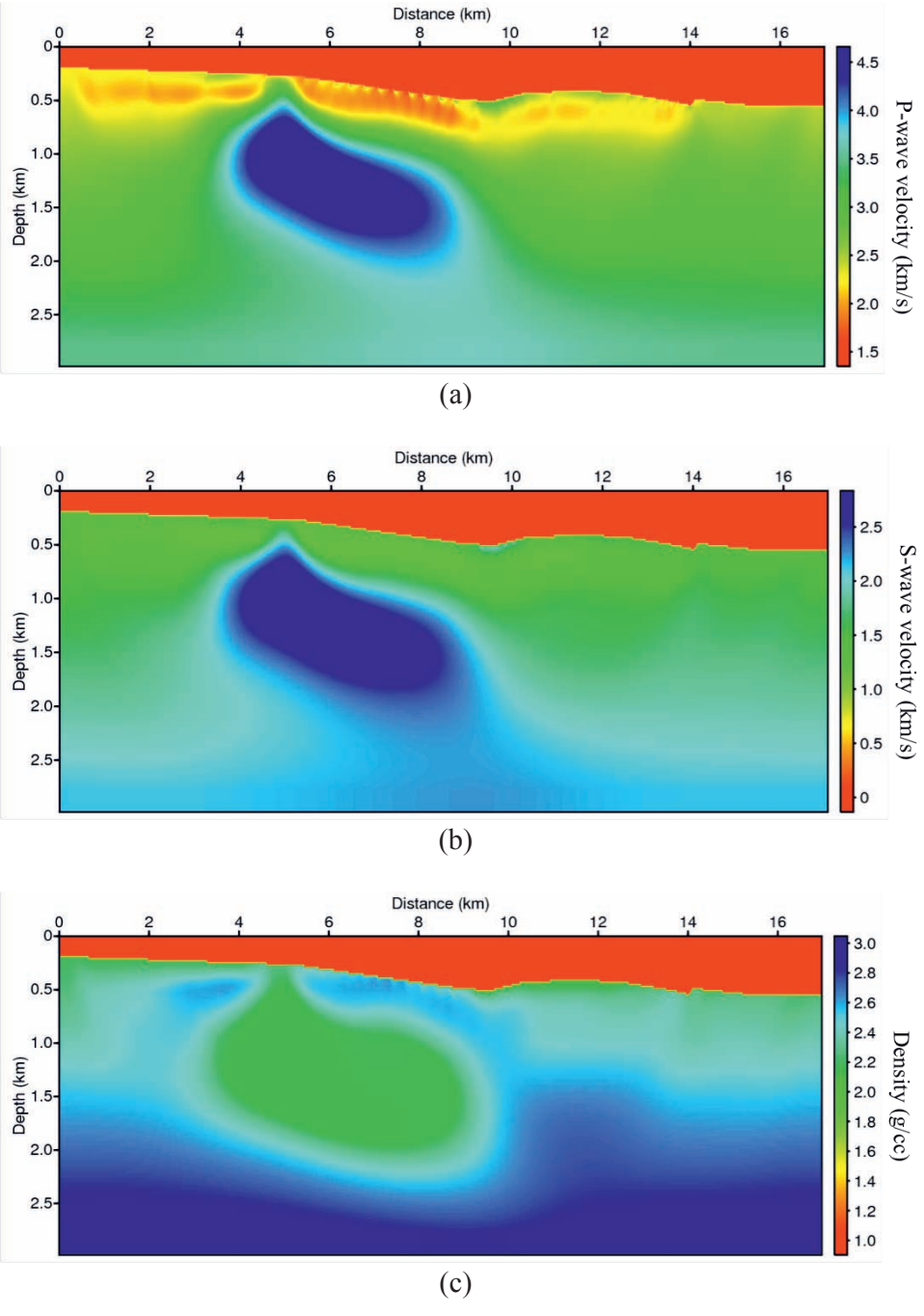

Fig. 4. Hess salt model reconstructed by Laplace-domain FWI after 200 iterations for acoustic-elastic coupled media using the conventional gradient: (a) V_P, (b) V_S, and (c) density.

In the final model computed using the conventional gradients after 200 iterations (Fig. 4), we estimate that V_P and V_S were properly reconstructed; however, high-density artefacts were generated immediately above the salt body. In our algorithm, a negative gradient indicates an increase in the value of the model parameters, whereas a positive gradient reduces the model parameters. In Figs. 3a and 3b, the gradients of the Lamé constants (λ and μ) show strong negative values in the salt body and high positive values immediately below the seafloor, respectively. In contrast, the conventional density gradient shows positive values in the salt body and negative values immediately below the seafloor (Fig. 3c). We think that this contrasting property caused the density artefacts in the final model (Fig. 4c).

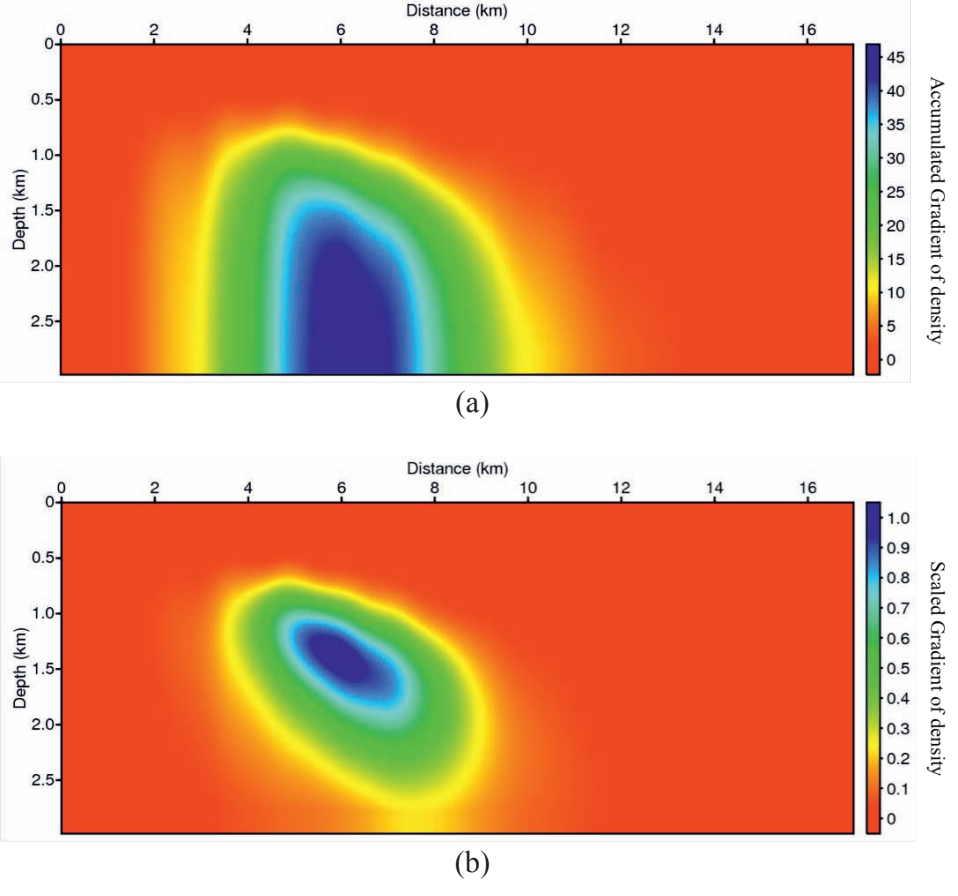

Fig. 5. (a) Accumulated and (b) scaled density gradients after 51 iterations.

The accumulated and scaled density gradients that were calculated by eqs. (14) and (15) after 51 iterations are shown in Fig. 5. Fig. 6 displays the final model computed by FWI using the scaled density gradient after 200 iterations. We find that V_P and V_S are almost the same as those in Fig. 4,

implying that V_P and V_S are estimated by both algorithms in a stable and consistent manner. Comparing Fig. 6c with Fig. 4c, however, we notice a recognizable difference in the final density models. Fig. 6c is obviously closer to the true model (Fig. 1c). In particular, the density artefact immediately below the seafloor was effectively removed. For a quantitative comparison, we plotted the density profiles at a depth of 3 and 7 km (Fig. 7), which shows a noticeable improvement in the density reconstruction using FWI with the scaled gradient over that with the conventional gradient. Bae et al. (2010) noted that it is difficult for FWI to properly recover the density because it is not sensitive enough to density. It appears that our empirical method for scaling the density gradient reconstructs the density more accurately than the conventional gradient method while simultaneously suppressing density artefacts in synthetic data test.

Real data example

We applied FWI with the scaled gradient to real data obtained in a sea area where a salt body is present below the seafloor. The data consist of 1,156 shots recorded on 804 receivers. The shot and receiver intervals are 37.5 m and 12.5 m, respectively, and the recording time is 15.0 s. Fig. 8 shows an example of shot gathers. Prior to FWI, the data were low-cut filtered, and all of the signals before the first arrival were muted (i.e., zeroed). Fig. 9 shows the initial V_P, Vs, and density models. In the initial model, V_P, V_S, and density in sea water were fixed to 1.5 km/s, 0 km/s, and 1.0 g/cc, respectively; whereas, below the seafloor, V_P increases linearly from 1.5 to 3.5 km/s, V_S increases from 0.9 to 2.5 km/s, and the density increases from 1.8 to 2.3 g/cc. We used 10 Laplace damping constants from 1 to 10. The grid size for the inversion was 25 m.

The final model sections after 200 iterations appear to reveal an object in the 1.5 to 2.5 km depth range (vertically) and in the 45 to 50 km distance range (horizontally) (Fig. 10). This object has higher V_P, V_S, and lower density than the surrounding material, which is representative of a salt structure embedded in the sediment. The reconstructed V_P and V_S values, well over 4 and 2 km/s, respectively, are typical of a salt dome. The reconstructed density values, less than 2.0 g/cc, are slightly lower than that of salt. However, the object estimated as a salt body is clearly distinguished in the density section. These features may indicate that FWI with the scaled gradient is adequate for defining a strong density contrast such as an embedded salt dome in the subsurface.

The density model, however, provides a better image of the salt structure than the V_P and V_S models. This may indicate that FWI with a scaled density gradient is adequate for defining a strong density contrast such as an embedded salt dome in the subsurface.

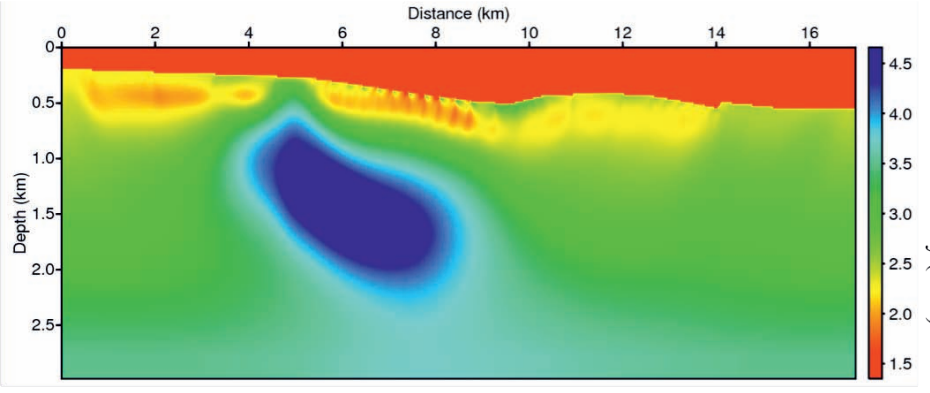

(a)

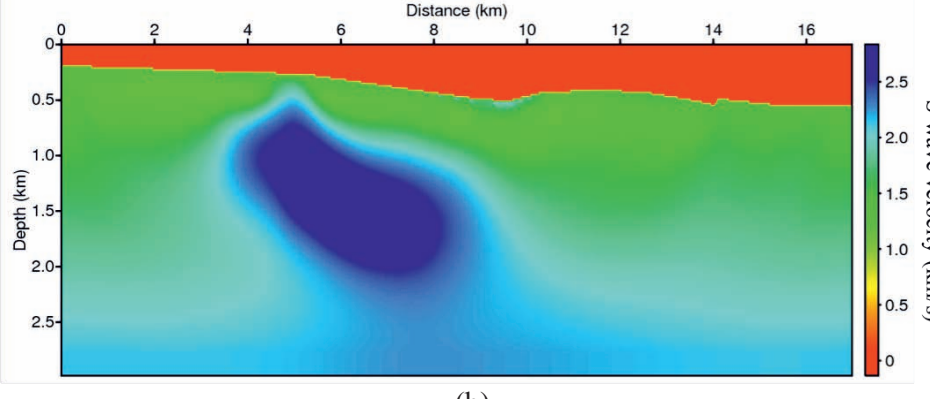

(b)

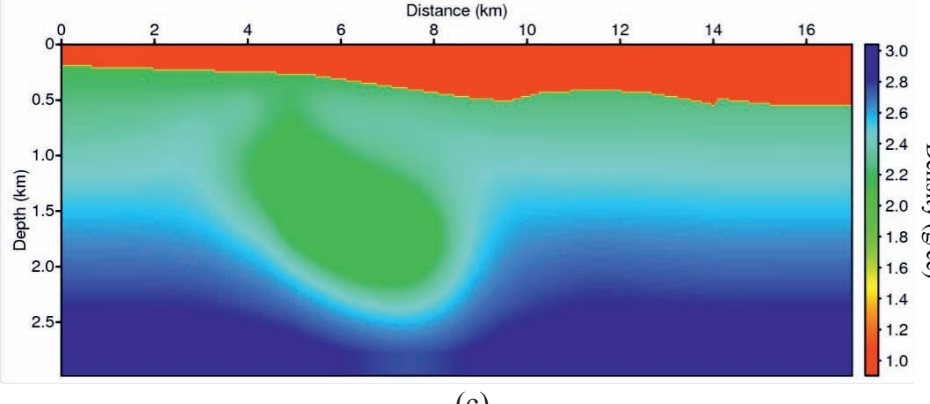

(c)

Fig. 6. Hess salt model reconstructed by Laplace-domain waveform inversion after 200 iterations for acoustic-elastic coupled media using the scaled density gradient: (a) V_P, (b) V_S, and (c) density.

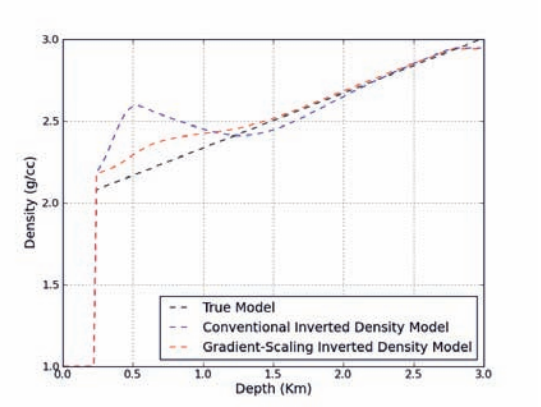

(a)

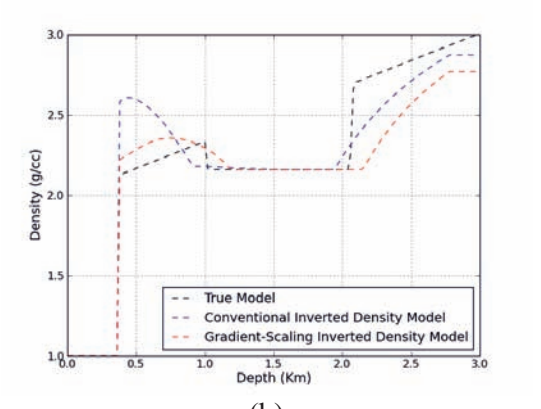

(b)

Fig. 7. Comparison of density profiles at distances of (a) 3 km and (b) 7 km.

Fig. 8. A portion of real shot gathers as an example of real seismic data.

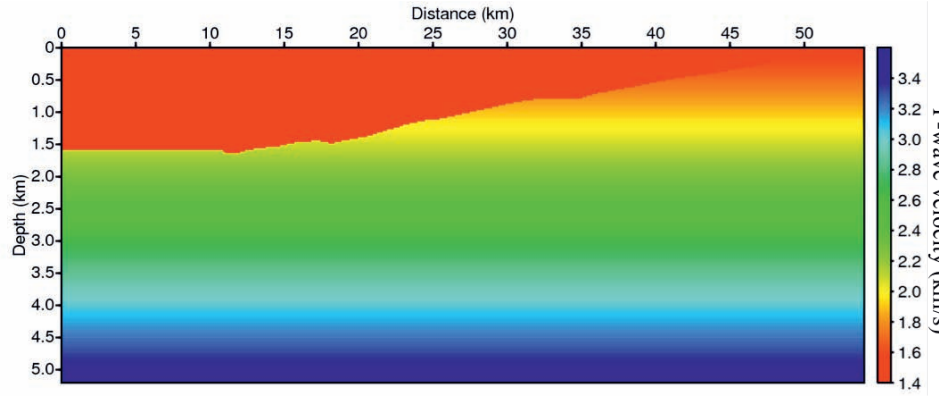

(a)

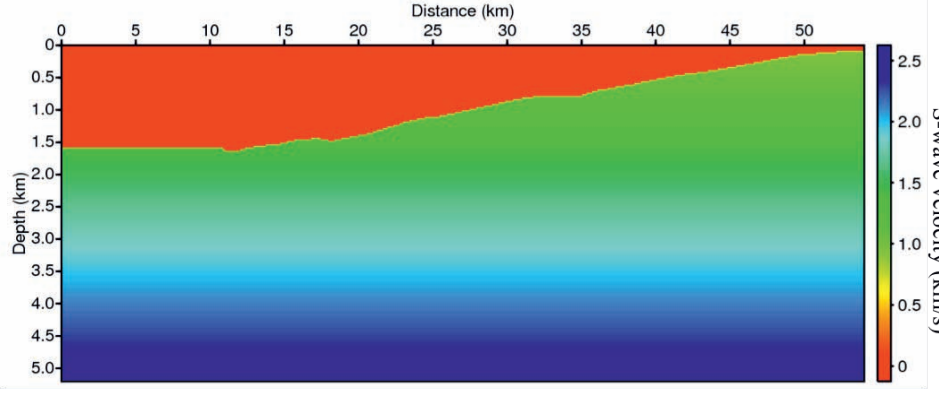

(b)

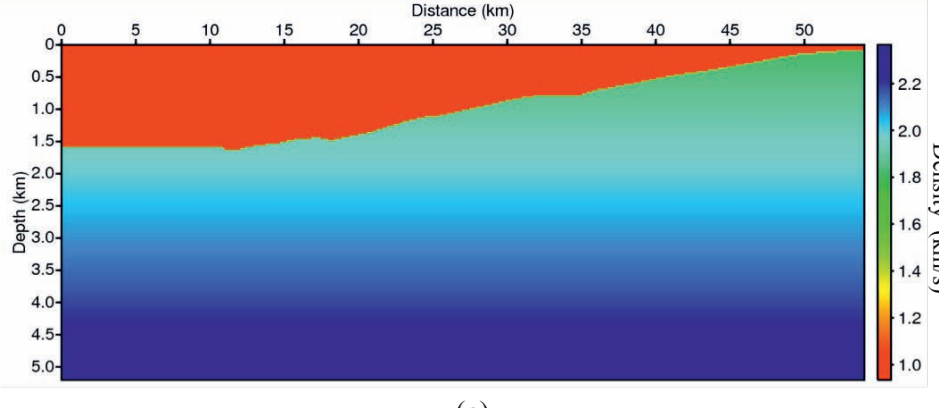

(c)

Fig. 9. Initial models for Laplace-domain waveform inversion of real data: (a) V_P, (b) V_S, and (c) density.

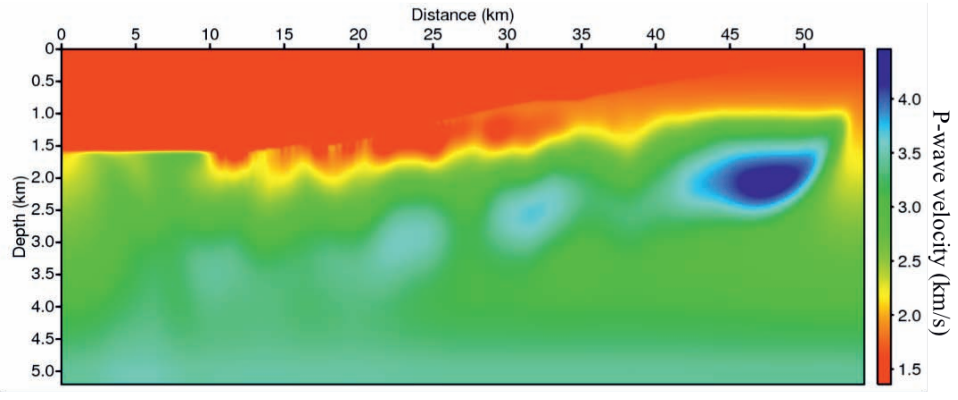

(a)

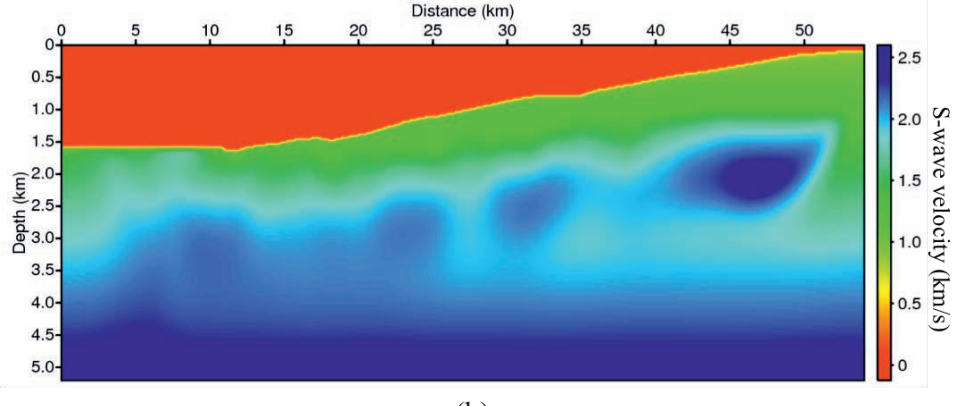

(b)

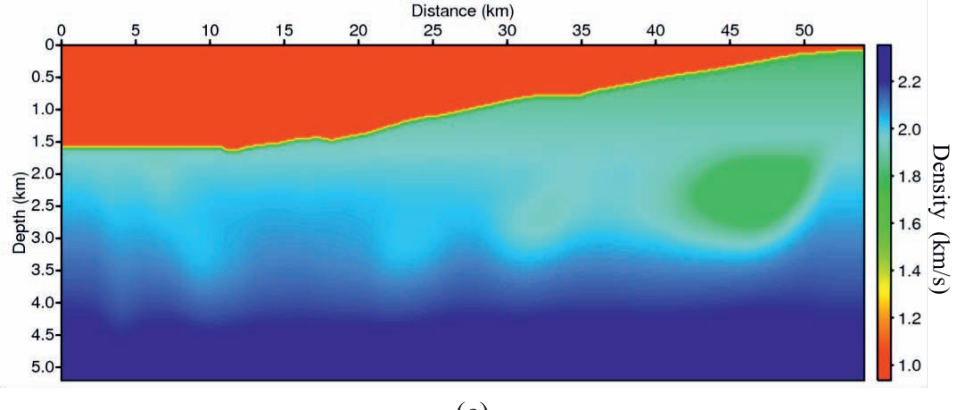

(c)

Fig. 10. Final models computed by Laplace-domain waveform inversion after 200 iterations for (a) V_P, (b) V_S, and (c) density. Note the presence of a salt body in the 40–50 km range, shown as a low density.

CONCLUSIONS

Waveform inversion cannot properly recover density because of its low sensitivity to density. In this study, we have presented a method for scaling the gradient of density for acoustic-elastic full-waveform inversion that improves the accuracy of reconstructed density. The gradient scaling is implemented by multiplying the conventionally computed gradient with the square of the gradient summed in the direction of depth. By applying this method for density inversion, we note that the gradient scaling method enables more accurate reconstruction of density properties for acoustic-elastic coupled media in inverted density model and better suppression of artefacts compared to the conventional gradient, particularly for a strong density contrast in synthetic and field data examples.

ACKNOWLEDGMENTS

This research was part of “Investigation of submarine resource environment and seabed methane release in the Arctic” research project, which is funded by the Korean Ministry of Oceans and Fisheries and by the Korea Polar Research Institute (PM18050).

REFERENCES

Bae, H.S., Shin, C., Cha, Y.H., Choi, Y. and Min, D.J., 2010. 2D acoustic-elastic coupled waveform inversion in the Laplace domain. Geophys. Prosp., 58: 997-1010.

Ha, T, Chung, W. and Shin, C., 2009. Waveform inversion using a back-propagation algorithm and a Huber function. Geophysics, 74: R15-R24.

Kang, S.G., Bae, H. and Shin, C., 2012. Laplace-Fourier domain waveform inversion for fluid-solid media. Pure Appl. Geophys., 169: 2165–2179.

Kang, S.G., Shin, C., Ha, W. and Hong, J.K., 2016. A gradient scaling method for Laplace domain full waveform inversion in acoustic-elastic coupled media. J. Seismic Explor., 25: 199-277.

Komatitsch, D., Barnes, C. and Tromp, J., 2000. Wave propagation near a fluid-solid interface: A spectral-element approach. Geophysics, 65: 623-631.

Pratt, R.G., Shin, C. and Hicks, G.J., 1998. Gauss-Newton and full Newton method in frequency domain seismic waveform inversion. Geophys. J. Internat., 133: 341-362.

Shin, C. and Min, D.J., 2006. Waveform inversion using a logarithmic wavefield. Geophysics, 71: R31-R42.

Shin, C., Pyun, S. and Bednar, J.B., 2007. Comparison of waveform inversion, part 1: conventional wavefield vs. logarithmic wavefield. Geophys. Prosp., 55: 449–64.

Shin, C. and Cha, Y.H., 2008. Waveform inversion in the Laplace domain. Geophys. J. Internat., 173: 922-931.

Shipp, R.M. and Singh, S.C., 2002. Two-dimensional full wavefield inversion of wide-aperture marine seismic streamer data. Geophys. J. Internat., 151: 325-344.

Symes, W., 2008. Migration velocity analysis and waveform inversion. Geophys. Prosp., 56: 765-790.

Tarantola, A., 1986. A strategy for nonlinear elastic inversion of seismic reflection data. Geophysics, 51: 1893-1903.

Zienkiewicz, O.C., Taylor, R.L. and Zhu, J.Z., 2005. The finite element method: its basis and fundamentals. Butterworth-Heinemann, Oxford.